Time to Line Crossing for Lane Departure Avoidance: A Theoretical Study and an Experimental Setting

Saïd Mammar, *Member, IEEE*, Sébastien Glaser, and Mariana Netto

Abstract—The main goal of this paper is to develop a distance to line crossing (DLC) based computation of time to line crossing (TLC). Different computation methods with increasing complexity are provided. A discussion develops the influence of assumptions generally assumed for approximation. A sensitivity analysis with respect to vehicle parameters and positioning is performed. For TLC computation, both straight and curved vehicle paths are considered. The road curvature being another important variable considered in the proposed computations, an observer for its estimation is then proposed. An evaluation over a digitalized test track is first performed. Real data are then collected through an experiment carried out in test tracks with the equipped proto-type vehicle. Based on these real data, TLC is then computed with the theoretically proposed methods. The obtained results outlined the necessity to take into consideration vehicle dynamics to use the TLC as a lane departure indicator.

Index Terms—Driver assistance, lane departure avoidance, observer, time to line crossing.

NOMENCLATURE

CG	Vehicle center of gravity.
m	Vehicle mass (1470 kg).
l_f	Distance from CG to front axle (1.00 m).
l_r	Distance from CG to rear axle (1.46 m).
l_v	Vehicle base length ($l_f + l_r = 2.46$ m).
a	Track width (1.40 m).
c_f	Front cornering stiffness (41.6 kN/rad).
c_r	Rear cornering stiffness (47.13 kN/rad).
β	Vehicle sideslip angle (radians).
r	Yaw rate (radians per second).
δ_f	Steering angle (radians).
y_G	Distance from lane centerline to CG (meters).
$y_{Gl}, (y_{Gr})$	Distance from the left (right) boundary of the lane to vehicle CG (meters).
$y_{ll}, (y_{lr})$	Distance from the left (right) boundary of the lane to front left tire (meters).
$y_{rl}, (y_{rr})$	Distance from the left (right) boundary of the lane to front right tire (meters).
ψ	Vehicle relative yaw angle (radians).
$\psi_L = \psi + \delta_f$	Front tire relative yaw angle (radians).
R_r	Road radius of curvature (meters).
R_v	Vehicle path radius of curvature (meters).
$R_{vl}, (R_{vr})$	Path radius of the front left (right) tire (meters).
$R_{v\lim_l}$	Maximal vehicle path radius for left boundary line crossing avoidance (meters).
$R_{v\lim_r}$	Maximal vehicle path radius for right boundary line crossing avoidance (meters).
D_{LC}	Distance to line crossing (meters).
t_{LC}	Time to line crossing (seconds).
L	Lane width (3.5 m).
v_l	Lateral speed (meters per second).
γ_l	Lateral acceleration (meters per second squared).

I. INTRODUCTION

TIME to line crossing (TLC) is defined as the time duration available for the driver before any lane boundary crossing. Several research studies outlined the importance of this indicator for both driver performance evaluation and lane departure characterization [5], [9]. Among the usual observations concerning TLC time evolution are the small TLC value periods prior to lane departure. This happens especially in case of driver drowsiness, which generally leads to a slow rate of TLC decreases with the possible presence of one or several TLC local minima corresponding to driver corrections. On the contrary, in case of vehicle loss control, the decreasing of TLC toward zero is generally faster [5], [13]. Unfortunately, real-time computation of TLC is not easy due to several limitations concerning availability of vehicle state variables, vehicle trajectory prediction, and lane geometry [16], [17]. Computation time is also a limiting factor. Thus, approximate formulas are used, the usual one being the ratio of lateral distance to lateral speed. This approximation has been successfully used in several works for lane departure systems evaluation [18]. While lateral speed cannot be easily observed, this formula is also not valid when the lateral speed varies [22]. A possible way to obtain TLC, which is developed in this paper, is to first compute the distance to line crossing (DLC) along the vehicle path and then divide it by the vehicle forward speed [13]. This approach, on one hand, presents the advantage to not use the lateral speed, which has to be estimated, but on the other hand requires a

long preview of the vehicle path and road geometry. The DLC-based computation method has been used in [21] assuming straight road geometry. However, vehicle path and road profile are both rarely straight and are a succession of curves to the right and left.

The purpose of this paper is to cover all aspects of TLC including human factors, theoretical, as well as real-data computation, highlighting at the same time parameter sensitivity. In Section II, TLC is positioned among other measures also used to study driver performance. In Section III, some useful geometric formulas of TLC are reviewed, first assuming the vehicle in stationary conditions without slipping, and then taking into account the understeering characteristic of the vehicle through a dynamic model in Section IV. Both straight and curved sections are considered, and several approximations that can be easily computed in real-time are provided. Finally, a linear dynamic model is used to predict future vehicle positions. An unknown input observer scheme is also proposed in this section to estimate the vehicle state and the road curvature, which are needed in the prediction phase. In Section V, an evaluation of the TLC is performed on straight and curved road sections. This evaluation is carried out on the basis of the established trigonometric formulas by considering several parameter variations. In Section VI, an experimental setting is proposed to collect real data for TLC computation. The evaluation is carried out on a 3.5-km-long digitalized test track that combines both straight and curved sections. It is shown that the observer is able to estimate the track curvature. We wrap up this paper in Section VII with the conclusions.

II. DRIVER COMMON MEASURES

In [11], where human–machine interaction (HMI) aspects are discussed, different sensory information useful for vehicle trajectory control while taking a bend are described. Two anticipation levels concerning these variables can be distinguished. The first level, long-term anticipation, begins as soon as the bend is visible. The second level, short-term anticipation and on-line control, begins just before and during bend taking.

Regarding long-term anticipation visual variables, one can cite the visual angle. This variable corresponds to the visual curvature of the road perceived by the driver and is available as soon as the bend is visible.

Concerning short-term anticipation, one can cite, for example, the optical flow. Changes in the optical flow directly specify interactions between the individual and the environment [4]. Some variables can be derived from the optical flow. A specific point in the optical flow, the tangent point, is one of them [10]. It is observed that, during bend taking, the driver tends to fix his view in this point. Another variable derived from the optical flow is the egocentric direction, which corresponds to the combination of extraretinal information concerning the direction of the gaze (with respect to the axis of the body) and the retinal location. Some studies indicate the utilization of the visual egocentric direction to guide displacements (see, for example, [12]).

Still talking about short-term anticipation, the TLC seems to play an important role as an indicator of steering performance
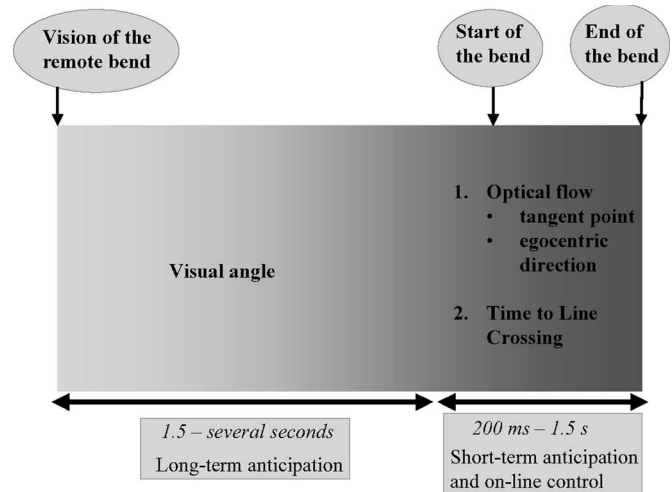

Fig. 1. Temporal representation of visual variables during bend taking.

as well as a regulating variable for the driver action (that is, it seems to help the driver's mind to perform the task of driving). With respect to the second case, research about TLC [14], [15] indicates that drivers can compensate for some errors of steering by decreasing their speed to maintain the TLC constant. In addition, the TLC seems to be a good indicator of the point at which the driver begins to use a strategy of open-loop visual steering (when he stops to look at the road momentarily to perform another task inside the vehicle), depending on the speed.

In addition to visual information, steering most certainly involves sensory information from various other organs, like vestibular, tactile, or proprioceptive organs.

Finally, in [11], it is highlighted that it is certainly not the same type of information used, depending on the temporality of the task. The question "assistance for what type?" is then raised. The temporal relation of the TLC with the other variables is shown in Fig. 1 (see [11]). Based on this temporal frame, we can distinguish two main classes of assistances: preventive or foresighted driving and short-term decision assistances. This division suggests that the first one would concern mainly informative or warning tasks to help the driver, while the second one could be based on warning as well as on active systems like trajectory correction. The task of driving in this case is mostly performed by the driver, and the controller acts for lane departure avoidance. The TLC fits this frame, being fundamental in helping to determine in which moment the assistance has to be turned on to avoid lane departure. In addition, its importance also appears in HMI studies for the drivers' trajectory evaluation.

III. GEOMETRIC EQUATIONS

In this section, the expressions for DLC and TLC are derived using a kinematic model of the car and trigonometric formulas. Straight and curved road sections are successively examined. In both cases, zero steering angle and constant nonzero steering angle are treated. Approximate solutions are provided to clarify the contribution to TLC of nonzero values of steering angle or road curvature.
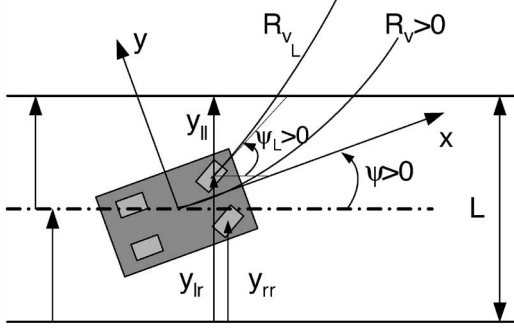
Fig. 2.   Common convention used for vehicle positioning.

A. Vehicle Positioning

We first derive the positioning of the vehicle front tires relative to the left and right lane boundaries according to the actual vehicle CG lateral displacement, vehicle geometry, and relative yaw angle. Fig. 2 summarizes all used conventions.

1) Positioning Relative to Left Lane Boundary: Assume that the vehicle CG is at a distance y_l from the left line of the lane of a straight road section with relative yaw angle ψ. Let y_{ll} (respectively y_{rl}) be the lateral distance of the front left (respectively right) tire to the line that would be crossed. The following equations hold for each front tire

$$\begin{cases} y_{ll} = y_l - l_f \sin\psi - \frac{a}{2}\cos\psi \\ y_{rl} = y_l - l_f \sin\psi + \frac{a}{2}\cos\psi. \end{cases} \quad (1)$$

All angles including relative yaw angle and steering angle are counted positive to the left (anti-clockwise). These formulas are still valid for a curved road section considering that the road radius R_r is much larger than y_l.

2) Positioning Relative to Right Lane Boundary: Similar formulas are obtained for the right lane boundary

$$\begin{cases} y_{lr} = y_r + l_f \sin\psi + \frac{a}{2}\cos\psi \\ y_{rr} = y_r + l_f \sin\psi - \frac{a}{2}\cos\psi. \end{cases} \quad (2)$$

Notice in addition that $y_r = L - y_l$, where L is the lane width. Also, when the front wheels steering angle δ_f is nonzero, the front tires' relative yaw angle is $\psi_L = \psi + \delta_f$.

B. Straight Road Section

1) Zero Steering Angle: Assuming that the steering angle is zero, the vehicle goes straight (Fig. 3). In case line crossing occurs on the left side of the lane, DLC is simply computed from

$$D_{\mathrm{LC}} = \frac{y_{ll}}{\sin\psi} = \frac{y_l - l_f\sin\psi - \frac{a}{2}\cos\psi}{\sin\psi}. \quad (3)$$

This formula is valid if ψ is positive. When ψ is negative, one has to use instead the vehicle front right tire distance from the right boundary of the lane (y_{rr}).

TLC is obtained by dividing D_{LC} by vehicle speed v. For a vehicle leaving on the left side of the lane, it is given by

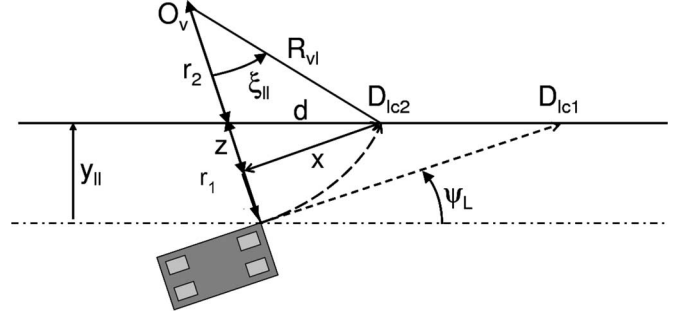$$t_{\mathrm{LC}} = \frac{y_{ll}}{v\sin\psi}. \quad (4)$$

Fig. 3.   DLC on straight road section using straight and circular vehicle paths.

Since $v\sin\psi = v_l$ is the lateral velocity, we have that $t_{\mathrm{LC}} = y_{ll}/v_l$, which is the common formula used in the literature [18].

We provide here another formula for TLC assuming that the lateral displacement is subject to a small constant acceleration γ_l, which appears during driver corrective maneuvers

$$t_{\mathrm{LC}} = \frac{1}{\gamma_l}\left(-v\sin\psi + \sqrt{(v^2\sin^2\psi + 2\gamma_l y_{ll})}\right). \quad (5)$$

The series expansion around $\gamma_l = 0$ gives

$$t_{\mathrm{LC}} = \frac{y_{ll}}{v\sin\psi}\left(1 - \frac{1}{2}\frac{y_{ll}}{v^2\sin^2\psi}\gamma_l\right) \quad (6)$$

which reduces to the former expression when $\gamma_l = 0$.

Let us now consider a vehicle circular path that corresponds to a constant nonzero steering angle.

2) Constant Steering Angle: The vehicle steering angle is now constant and positive nonzero and is equal to δ_{f0}. In steady state, the front left tire path is a circle arc of radius R_{v_l} such that

$$R_{v_l} = \frac{l_v}{\tan\delta_{f0}} - \frac{a}{2} = \frac{v}{\dot\psi} - \frac{a}{2} \quad (7)$$

where l_v is the vehicle base length and $\dot\psi$ is the yaw rate. Notice that, as indicated above, the front left tire presents a relative yaw angle of $(\psi_L = \psi + \delta_{f_0})$.

The DLC is obtained from the following process:
1) Compute $r_1 = y_{ll}/\cos\psi_L$ and $r_2 = R_{v_l} - r_1$ (Fig. 3).
2) Compute the distance d from

$$d = r_2\sin\psi_L + \sqrt{R_{v_l}^2 - r_2^2\cos^2\psi_L}. \quad (8)$$

3) Compute the angle ξ_{ll} as

$$\xi_{ll} = \cos^{-1}\left(\frac{r_2^2 + R_{v_l}^2 - d^2}{2R_{v_l}r_2}\right). \quad (9)$$
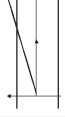
Finally, DLC is obtained as

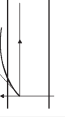$$D_{\mathrm{LC}} = \xi_{ll}R_{v_l}. \quad (10)$$

When $\psi_L = 0$, the previous equations reduce to $r_1 = y_{ll}$, $r_2 = R_{v_l} - y_{ll}$, $d = \sqrt{R_{v_l}^2 - r_2^2}$, and $\xi_{ll} = \cos^{-1}(r_2/R_{v_l})$.

The previous equations are established using distance formulas. It is, however, possible to obtain more simple equations. According to Fig. 3, $\sin\psi_L = z/d$, $\cos\psi_L = x/d$,

TABLE I
SUMMARY OF TLC FOR LEFT LINE ON STRAIGHT ROAD SECTION
WHERE $R_{v_{\lim_l}} = ((-y_{ll} + a\cos\psi)/(1 - \cos\psi_L)) < 0$,
$R_{v_{\lim_r}} = (L - (y_{ll} + a\cos\psi))/(1 - \cos\psi_L)$, AND
$\xi_{lr} = \cos^{-1}(\cos\psi_L - (y_{ll}/R_{v_l})) + \psi_L$

	$\delta_f = 0,$ $\psi > 0$	$\delta_f > 0,$ $\psi_L > 0$	$\delta_f > 0,$ $\psi_L < 0$	$\delta_f < 0,$ $\psi_L > 0$
Case				
R_{v_l}	∞	$\dfrac{l_v}{\tan\delta_{f0}} - \dfrac{a}{2}$	$< R_{v_{\lim_r}}$	$< R_{v_{\lim_l}}$
TLC	$\dfrac{y_{ll}}{v\sin\psi}$	$\dfrac{R_{v_l}}{v}\xi_{ll}$	$\dfrac{R_{v_l}}{v}\xi_{ll}$	$-\dfrac{R_{v_l}}{v}\xi_{lr}$

$\cos\xi_{ll} = (r_2 + z)/R_{v_l}$, and $\sin\xi_{ll} = x/R_{v_l}$. Combining the four previous equations leads to

$$\xi_{ll} = \cos^{-1}\left(\cos\psi_L - \frac{y_{ll}}{R_{v_l}}\right) - \psi_L. \quad (11)$$

If ψ_L and δ_f are both negative, the lane departure should occur on the right side of the lane. The formulas in this case are similar, but lateral displacement has to be taken relative to the right lane at the point of contact of the front right wheel.

Suppose now that ψ_L and δ_f are of opposite sign, as when the driver performs a recovering maneuver. In such a case, the vehicle may first leave the line on one side and then come back to the lane and finally cross the line on the other side. However, there exists a relation between R_{v_l}, y_{ll}, ψ_L, and the lane width L that determines if the first lane departure will occur on one side or on the other. When $\psi_L < 0$ and $\delta_f > 0$, the vehicle path radius has to be under a limit value $R_{v_{\lim_r}} > 0$ so that lane departure occurs on the left side. Similarly, when $\psi_L > 0$ and $\delta_f < 0$, the vehicle path radius has to be also under a limit value $R_{v_{\lim_l}} < 0$ so that lane departure still occurs on the left side.

Table I summarizes cases of TLC calculation when lane departure is expected on the left border.

In this table, $[R_{v_{\lim_l}} = ((-y_{ll} + a\cos\psi)/(1 - \cos\psi_L)) < 0$, $R_{v_{\lim_r}} = (L - (y_{ll} + a\cos\psi))/(1 - \cos\psi_L)$, and $\xi_{lr} = \cos^{-1}(\cos\psi_L - (y_{ll}/R_{v_l})) + \psi_L]$.

A similar table can be drawn up for the lane departure expected on the right side.

C. Constant Radius Curved Road Section

1) Zero Steering Angle: Suppose now that the vehicle is on a curved road section of radius R_r. The steering is zero such that the vehicle continues its trajectory in the direction of its longitudinal axis.

Assuming that the lane departure occurs on the left side of the lane (Fig. 4), the computation of D_{LC} is straightforward. One may obtain

$$D_{LC} = (R_r + y_{ll})\sin\psi - \sqrt{R_r^2 - (R_r + y_{ll})^2\cos^2\psi}. \quad (12)$$

This solution exists if and only if $\cos\psi \le (R_r/(R_r + y_{ll}))$. Otherwise, lane departure occurs on the right side of the lane
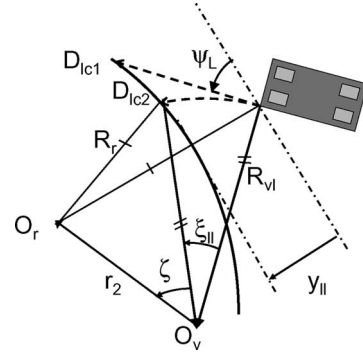

Fig. 4. Vehicle on curved road section with zero and nonzero steering angles.

and D_{LC} is given in this case by

$$D_{LC} = (R_r + y_{ll} + a\cos\psi)\sin\psi$$
$$+ \sqrt{(R_r + L)^2 - (R_r + y_{ll} + a\cos\psi)^2\cos^2\psi}. \quad (13)$$

It is important to notice that on straight road section, when $\delta_f = 0$, the sign of ψ determines the side of the lane where the lane departure occurs. On a curved road section, right side lane departure may occur even if ψ is positive.

Useful approximate formulas that highlight the effect of road radius of the curvature on the DLC, when the radius of curvature goes to infinity, can be derived.

- Lane departure on the left side assuming $\psi > 0$

$$D_{LC} \approx \frac{y_{ll}}{\sin\psi} + \frac{1}{2}\left(\frac{\cot^2\psi}{\sin\psi}\right)y_{ll}^2\frac{1}{R_r}. \quad (14)$$

- Lane departure on the right side assuming $\psi \le 0$

$$D_{LC} \approx \frac{y_{rr}}{\sin\psi} - \frac{1}{2}\left(\frac{\cot^2\psi}{\sin\psi}\right)y_{rr}^2\frac{1}{R_r}. \quad (15)$$

Supposing that $\psi = 0$, then the lane departure will occur on the right side of the lane if the road goes to the left. DLC is $D_{LC} = \sqrt{(L - y_{ll})(y_{ll} + L + 2R_r)}$ and TLC is $t_{LC} = \sqrt{(L - y_{ll})(y_{ll} + L + 2R_r)}/v$. On the other hand, at the initial time, the vehicle lateral acceleration is $\gamma_l = v^2/(R_r + y_{ll}) = (v^2/R_r)(1/(1 + (y_{ll}/R_r))) \approx (v^2/R_r)$. This leads to the equality

$$t_{LC} = \frac{\sqrt{R_r}}{v}\sqrt{(L - y_{ll})\left(2 + \frac{y_{ll} + L}{R_r}\right)} \quad (16)$$

or assuming $R_r \gg (y_{ll} + L)$

$$t_{LC} \approx \sqrt{\frac{2(L - y_{ll})}{\gamma_l}}. \quad (17)$$

This formula is similar to that for time to collision t_c with an obstacle located at a distance d when the vehicle has a constant braking deceleration of γ_b, i.e., $t_c = \sqrt{2d/\gamma_b}$.

Tables II and III summarize all formulas for lane departure on the left and right sides. All cases of positive and negative road radius of curvature and vehicle yaw angle errors are covered.

TABLE II
SUMMARY OF TLC FOR LEFT LINE ON CURVED ROAD SECTION
ASSUMING STRAIGHT VEHICLE PATH

Case	$R_r > 0$, $\psi_L > \psi_{tl}$	$R_r > 0$, $\psi_L = \psi_{tl}$	$R_r < 0$, $\psi_L \geq \psi_{tr}$
TLC	$\dfrac{D_1}{v}$	$\dfrac{\sqrt{2y_{ll}c_1}}{v}$	$\dfrac{D_2}{v}$

TABLE III
SUMMARY OF TLC FOR RIGHT LINE ON CURVED ROAD SECTION
ASSUMING STRAIGHT VEHICLE PATH

Case	$R_r < 0$, $\psi_L < \psi_{tr}$	$R_r < 0$, $\psi_L = \psi_{tr}$	$R_r > 0$, $\psi_L \leq \psi_{tl}$
TLC	$\dfrac{D_3}{v}$	$\dfrac{\sqrt{-2y_{rr}c_2}}{v}$	$\dfrac{D_4}{v}$

In these tables, $D_1 = c_1 \sin \psi - \sqrt{R_r^2 - c_1^2 \cos^2 \psi}$, $D_2 = c_2 \sin \psi + \sqrt{R_r^2 - c_2^2 \cos^2 \psi}$, $D_3 = c_2 \sin \psi - \sqrt{c_3^2 - c_2^2 \cos^2 \psi}$, and $D_4 = c_4 \sin \psi + \sqrt{c_3^2 - c_4^2 \cos^2 \psi}$. $c_1 = R_r + y_{ll}$, $c_2 = R_r + L + y_{rr}$, $c_3 = R_r + L$, and $c_4 = R_r + y_{rl}$. The angles ψ_{tr} and ψ_{tl} are computed as $\psi_{tr} = -\cos^{-1}((R_r + L)/(R_r + L - y_{rr}))$ and $\psi_{tl} = \cos^{-1}(R_r/(R_r + y_{ll}))$.

2) Constant Steering Angle: According to Fig. 4, the arc length is given by $D_{LC} = R_{v_l}\xi_{ll}$. Computation of ξ_{ll} is, however, different in this case. It is achieved by the following process (see Fig. 4):

• The distance r_2 between the center point of the road curve and the center point of the vehicle path is given by

$$r_2 = \sqrt{(R_r + y_{ll})^2 + R_{v_l}^2 - 2(R_r + y_{ll})R_{v_l}\cos\psi}. \quad (18)$$

• The angle ζ is then computed as

$$\zeta = \cos^{-1}\left(\frac{R_{v_l}^2 + r_2^2 - R_r^2}{2r_2 R_{v_l}}\right). \quad (19)$$

• Finally, the angle ξ_{ll} is given by

$$\xi_{ll} = -\zeta + \cos^{-1}\left(\frac{r_2^2 + R_{v_l}^2 - (R_r + y_{ll})^2}{2r_2 R_{v_l}}\right). \quad (20)$$

In the previous computation, it has been assumed that both ψ_L and δ_f are positive and that the lane departure occurs on the left side. However, this lane departure may not occur on the left side even in this case. The limit situation is when the path of the vehicle is tangent to the left border of the lane (Fig. 5). In such a case, the angle ζ is equal to zero and the two circle centers O_v and O_r are aligned and the distance between them is $r_2 = R_{v_l} - R_r \geq 0$. The corresponding limit value $R_{v_{\lim_l}}$ of R_{v_l} is given by

$$R_{v_{\lim_l}} = \frac{1}{2}\frac{\left(2 + \frac{y_{ll}}{R_r}\right)y_{ll}}{-1 + \left(1 + \frac{y_{ll}}{R_r}\right)\cos\psi_L}. \quad (21)$$
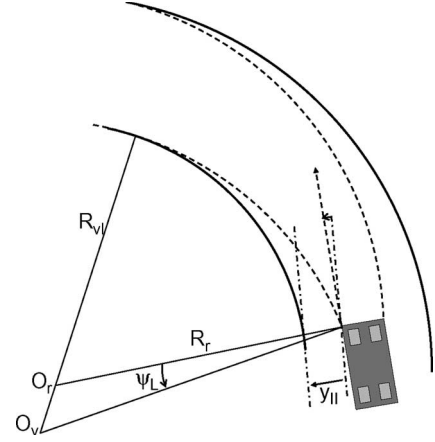

Fig. 5.   Limit trajectory for curved road section.

TABLE IV
SUMMARY OF TLC FOR LEFT LINE ON CURVED ROAD SECTION

Case	$\delta_f = 0$, $\cos\psi_L < \frac{R_r}{R_r + y_{ll}}$ $\psi_L > 0$	$\delta_f = \delta_{f0} > 0$, $\cos\psi_L < \frac{R_r}{R_r + y_{ll}}$	$\delta_f = \delta_{f0} > 0$, $\cos\psi_L > \frac{R_r}{R_r + y_{ll}}$
R_{v_l}	∞	$R_{v_l} = \frac{l_v}{\tan\delta_{f0}} - \frac{a}{2}$ $< R_{v_{\lim_l}}$	$R_{v_{\lim_l}} < R_v$ $R_v < R_{v_{\lim_r}}$
TLC	$\frac{1}{v}\left(\frac{(R_r + y_{ll})\sin\psi -}{\sqrt{R_r^2 - (R_r + y_{ll})^2\cos^2\psi}}\right)$	Use equation (20)	∞

TABLE V
SUMMARY OF TLC FOR RIGHT LINE ON CURVED ROAD SECTION

Case	$\delta_f = 0$, $\psi_L \geq 0$, $\cos\psi_L > \frac{R_r}{R_r + y_{ll}}$	$\delta_f = \delta_{f0} > 0$, $\cos\psi_L > \frac{R_r}{R_r + y_{ll}}$	$\delta_f > 0$
R_{v_r}	∞	$R_{v_r} = \frac{l_v}{\tan\delta_{f0}} - \frac{a}{2}$ $R_{v_r} > R_{v_{\lim_r}}$	$R_{v_r} > R_{v_{\lim_l}}$ $R_{v_r} < R_{v_{\lim_r}}$
TLC	A	similar to (20)	∞

Note that this is only possible for $\psi_L < \cos^{-1}(R_r/(R_r + y_{ll}))$. In this case, the steering angle has to be less than $\tan^{-1}(l_v/R_{v_{\lim_l}})$ to avoid a lane departure on the left.

Assume now that ψ_L and δ_f are of opposite signs. Without loss of generality, we consider the case when $\psi_L < 0$ and $\delta_f > 0$, and we determine the condition to avoid lane departure on the right side. The limit value $R_{v_{\lim_r}}$ of R_v is

$$R_{v_{\lim_r}} = \frac{1}{2}\frac{L\left(2 + \frac{L}{R_r}\right) - y_{rl}\left(2 + \frac{y_{rl}}{R_r}\right)}{\left(1 + \frac{L}{R_r}\right) - \left(1 + \frac{y_{rl}}{R_r}\right)\cos\psi_L}. \quad (22)$$

When the vehicle path radius verifies $R_{v_{\lim_l}} < R_v < R_{v_{\lim_r}}$, TLC is infinite since the vehicle trajectory always remains within lane boundaries.

Table IV summarizes cases of TLC calculation when the lane departure is expected on the left border. The road curvature is assumed positive, which means that the bend is also oriented to the left.

Similarly, Table V corresponds to the right side when the bend is still oriented to the left.

In Table V, $A = (1/v)\left((R_r + y_{ll} + a\cos\psi_L)\sin\psi_L + \sqrt{(R_r + L)^2 - (R_r + y_{ll} + a\cos\psi_L)^2\cos^2\psi_L}\right)$. In Tables IV and V, only nonnegative values of δ_f are given; however, similar results may be obtained for negative steering angles by

providing some substitutions. Analogous results may also be obtained for curved road sections to the right ($R_r < 0$).

D. Kinematic Prediction of Vehicle Trajectory

Suppose that the road curvature is made available by the use of an observer for example. Using the lateral positioning and relative yaw angle obtained by the video sensor together with the yaw rate sensor, the steering angle, and the speed, it is possible to apply the formula established in Section III. The process has to pass through the tables listed above to determine in which particular case the vehicle is. It is also possible to perform vehicle future position prediction assuming circular paths. An associated kinematic model that neglects vehicle slip motion can be used. It is given by ($\dot{x}_v = v \cos\theta$, $\dot{y}_v = v \sin\theta$, $\dot{\theta} = v/(l_f + l_r)\tan\delta_f$), where θ is the vehicle heading angle, l_f and l_r are, respectively, the distance from the vehicle CG to the front and rear axles, and (x_v, y_v) are the vehicle global coordinates. The relative yaw angle dynamics is $\dot{\psi} = \dot{\theta} - v/R_{r \cos\psi}$.

Practically, from CG lateral deviation and relative yaw angle, we determine the front tires' path radius and relative yaw angle. As the first concern is to know if TLC is higher than the threshold S, one first generates for each of the front tires a circular arc of length $(Si/N)v(i = 1, \ldots, N)$, where N is the number of desired samples. The two lateral deviations are computed for each sample. If, until the Nth sample, they are within the lane limits, TLC is thus higher than S and the procedure stops. Otherwise, if at time sample k the lateral deviation is found beyond the lane limits, this means that the lane boundary has been crossed between $(k-1)$ and k, the minimal TLC is thus $(S(k-1)/N)$. A refinement is possible to obtain a better approximation by using resampling within the time interval $[S(k-1)/N, Sk/N]$.

Notice that the procedure may be accelerated if a straight vehicle path is assumed. An initial line segment of length Sv/N can then be directly generated, and lateral deviations are first computed for the last points of the arcs. Thus, iteration may be done backward if one is found beyond the boundaries of the lane. Otherwise, we can conclude that TLC is higher than S seconds with only two lanes positioning.

In the following, the effect of vehicle dynamics on TLC computation is examined. An unknown input proportional multiple integral observer is proposed for vehicle state and road curvature estimation.

IV. PREDICTION USING DYNAMIC MODELS

A. Vehicle Models

Several models can be used for numerical TLC estimation on various road types. For high longitudinal speeds assuming small angles, a dynamic bicycle linear model can be used. It is formulated in terms of lateral displacement and lateral speed [1]. This model is well fitted for motorway driving conditions. First of all, the lateral acceleration written in the road frame is given by

$$\ddot{y}_G = \gamma_l - v\frac{1}{R_r} = \dot{v}_l - v^2 \rho_r \qquad (23)$$

where $\rho_r = R_r^{-1}$ is the road curvature.

The vehicle path radius R_{v_d} of this dynamic model is thus

$$R_{v_d} = \frac{(l_f + l_r)}{\delta_{f_0}}(Kv^2 + 1) \qquad (24)$$

where $K = (l_r c_r - l_f c_f)m/c_f c_r(l_r + l_f)^2$ is a stabilizing factor, m is the vehicle mass, and c_f and c_r are, respectively, the front and rear tires cornering stiffness. The factor K is positive for an understeered vehicle, negative for an oversteered vehicle, and zero for a neutral vehicle. The path radius $(R_{v_l} = (l_f + l_r)/\tan\delta_{f_0} \approx (l_f + l_r)/\delta_{f_0})$ obtained with the kinematic model has thus to be corrected.

The temporal relation between the lateral acceleration γ_l, the lateral speed v_l, the yaw rate r, and the steering angle δ_f is

$$\gamma_l = -\frac{(c_f + c_r)}{mv}v_l + \frac{1}{v}\frac{(c_r l_r - c_f l_f)}{m}r + \frac{c_f}{m}\delta_f. \qquad (25)$$

Under the assumption $v_l \approx v\beta$, which holds for lateral acceleration under 0.3 g, one can notice that the contribution of the yaw rate to lateral acceleration decreases when the speed increases in favor of the sideslip angle. This means that the vehicle tends to slip rather than to revolve. Thus, the computational method of TLC has to be changed.

In addition to the previously established trigonometric formulas, the following formulas can be used for the computation of TLC. Only left lane departure cases are provided.

- If lateral speed and lateral acceleration are available for measurement, the first approximate formula that can be used on straight road sections is

$$t_{\text{LC}} = \frac{-v_l + \sqrt{v_l^2 + 2\gamma_l y_{ll}}}{\gamma_l}. \qquad (26)$$

  This formula is simply derived from the lateral motion of the vehicle assumed to be at a constant lateral acceleration γ_l with the initial lateral speed v_l.

- On straight road section approximation, taking into account nonzero steering angle

$$t_{\text{LC}} = \frac{l_v(Kv^2 + 1)\cos^{-1}\left(\cos\psi - \frac{y_{ll}}{l_v(Kv^2+1)}\delta_{f_0}\right) - \psi}{v\delta_{f_0}}. \qquad (27)$$

  This equation is simply derived from the previously trigonometric equation (10) obtained for nonzero steering angle on a straight road section, where the vehicle path is replaced in this case by the dynamic one (see Table III).

- On a curved section, with nonzero steering angle, the possible equation is

$$t_{\text{LC}} = \frac{-v\sin(\psi + \delta_{f_0}) + \sqrt{v^2\sin^2(\psi + \delta_{f_0}) + 2v^2\left(\frac{1}{R_{v_d} - \frac{a}{2}} - \frac{1}{R_r}\right)y_{ll}}}{v^2\left(\frac{1}{R_{v_d} - \frac{a}{2}} - \frac{1}{R_r}\right)}$$

$$\qquad (28)$$

This equation is similar to (26), in which $v \sin(\psi + \delta_{f_0})$ is the lateral speed, and $v^2(1/(R_{v_d} - a/2) - 1/R_r)$ is the lateral acceleration relative to the road.

B. Lateral Speed and Curvature Estimation

The bicycle model presents a state vector x with four state variables. The state variables are the lateral speed, the lateral displacement, the relative yaw angle, and the yaw rate. Only the three last variables are available for measurement. In addition, the road curvature affects the system as an unknown input [1], i.e.,

$$\begin{cases} \dot{x} = Ax + B\delta_f + E\rho_r \\ y = Cx. \end{cases} \tag{29}$$

An observer can be designed to achieve both state and unknown input estimations. In [8], a second-order polynomial model of the road is assumed in the vehicle coordinates. A discrete-time Kalman filter observer is then synthesized for both lateral velocity estimation and polynomial model coefficients estimation. Another Kalman filter that considers the road bank angle but ignores the road geometry in terms of curvature variation is also presented in [20]. Here, it is assumed that the road curvature is almost constant or affine varying, and we choose a proportional two-integral (P2I) observer that is able to estimate the curvature and its derivative. The road curvature is considered as an unknown input ρ_r [7]. The P2I observer has the form

$$\begin{cases} \dot{\hat{x}} = A\hat{x} + B\delta_f + L_p(y - \hat{y}) + E\hat{\rho}_{r_2} \\ \dot{\hat{\rho}}_{r_2} = \hat{\rho}_{r_1} + L_{i_2}(y - \hat{y}) \\ \dot{\hat{\rho}}_{r_1} = L_{i_1}(y - \hat{y}). \end{cases} \tag{30}$$

The second equation describes the integral loop gain added to the proportional one in the first equation. The matrix gains L_p, L_{i1}, and L_{i2} are determined in such a way to enable asymptotic convergence to zero of the state estimation error, the unknown input estimation errors, and the estimation error of the derivative of the unknown input respectively defined by $e = x - \hat{x}$, $e_{\rho_2} = \rho_r - \hat{\rho}_{r_2}$, and $e_{\rho_1} = \dot{\rho}_r - \hat{\rho}_{r_1}$. This is achieved by making the Hurwitz matrix

$$\begin{bmatrix} A & E & 0 \\ 0 & 0 & 1 \\ 0 & 0 & 0 \end{bmatrix} - \begin{bmatrix} L_p \\ L_{i_2} \\ L_{i_1} \end{bmatrix} \begin{bmatrix} C & 0 & 0 \end{bmatrix}. \tag{31}$$

Thus, any eigenvalue assignment method can be applied to obtain the matrix gain $[L_p \; L_{i_2} \; L_{i_1}]$.

C. Prediction of Vehicle Future Positions

For vehicle future positions dynamic prediction, the model (29) has to be transformed into a discrete-time model using the Tustin method. Prediction is performed during the time range in the frame attached to the road. This frame is obtained by the orthogonal projection of the vehicle CG on the lane centerline. This discrete model is of the form $x_{k+1} = \Phi x_k + \Gamma v_k$, where $x_k = [y_G, \dot{y}_G, \psi, \dot{\psi}]^T$ and $v_k = [\delta_f, \rho]^T$.
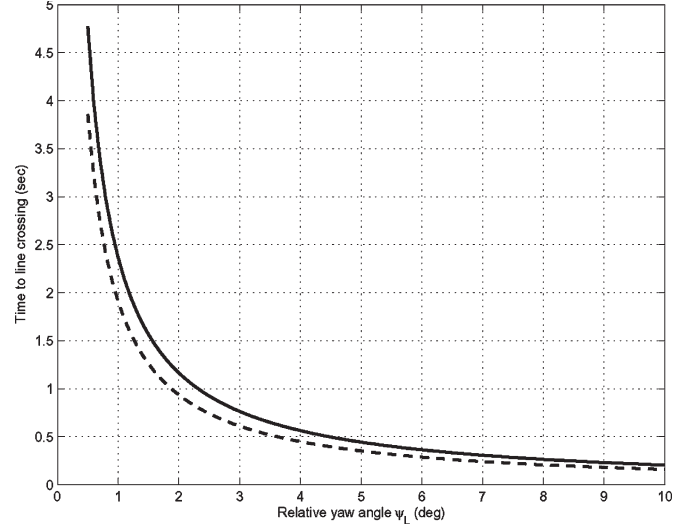

Fig. 6.　TLC versus relative yaw angle for a fixed speed of 90 km/h on straight road section and zero steering angle.

This model is initialized using the observer estimation values for both state and road curvatures [8]. This prediction is generally of high computation and time consuming; it is only necessary in cases where vehicle dynamics are far from steady-state values and positioning values are critical. Prediction is performed until one of the vehicle front wheels reaches the lane edge or the fixed limit of time prediction has been completed [2], [3].

In the following, the established trigonometric formulas are investigated to highlight the effects of variables appearing in the different formulas on the achieved TLC. Particularly, limits on the acceptable relative yaw angle and lateral acceleration for minimum TLC values are outlined.

V. SIMULATION ANALYSIS

A. Analysis With Zero Steering Angle on Straight Road Section

It is generally assumed that the driver's accuracy during lane keeping maneuvers is about 20 cm around the lane centerline at the vehicle center of gravity. On the other hand, lane departures occur with a relative yaw angle under 6°. Let us define $d_m = \pm 20$ cm. Supposing that ψ is positive, the lane departure will occur on the left side, and the point of interest is the front left tire contact with the road. Vehicle geometry influences the lateral displacement of this point. This displacement is half the wheel base at zero relative yaw angle and increases at about 17 cm when the relative yaw angle is 10°. The point is located at a distance $(d_m + l_f \sin \psi + (a/2) \cos \psi)$ from the lane centerline with $l_f = 1$ m and $a = 1.4$ m. To maintain a TLC of $t_{\min} = 2$ s for a given speed v, from (3), the relative yaw angle has to be under $\psi_{\max}$ given by

$$\psi_{\max} = -\phi + \sin^{-1}\left(\frac{\frac{L}{2} - d_m}{\sqrt{(vt_{\min} + l_f)^2 + \frac{a^2}{4}}}\right) \tag{32}$$

where the angle ϕ is such that $\sin \phi = (a/2)/\sqrt{(vt_{\min} + l_f)^2 + (a^2/4)}$.
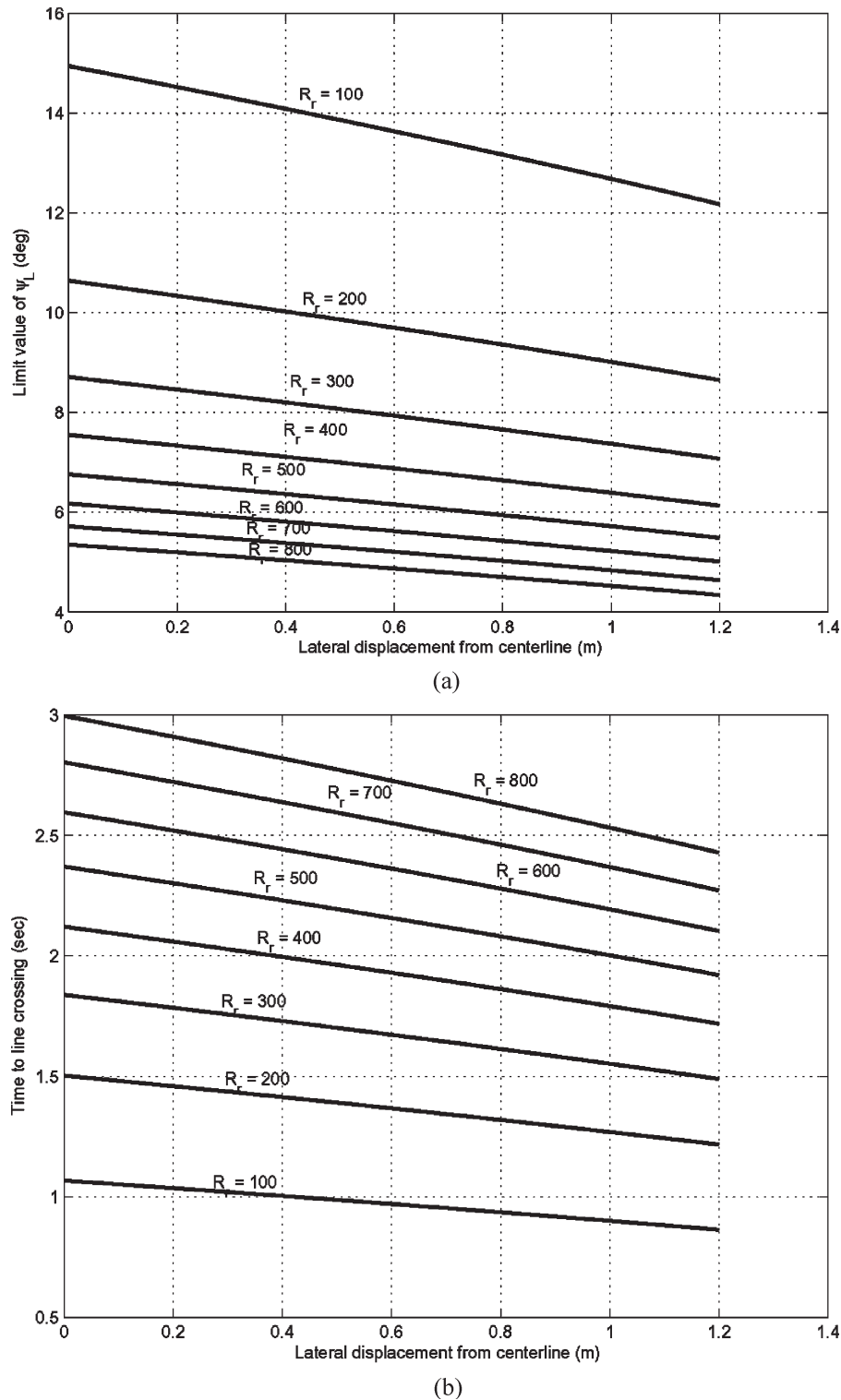
(a)

(b)

Fig. 7.   (a) Limit values of ψ_L as a function of the lateral displacement for different road radius of curvature. (b) TLC values obtained with the maximum value of ψ_L as a function of the lateral displacement for different road radius of curvature.

The relative yaw angle has to be under $2°$ for speeds greater than 45 km/h, and only $1°$ is acceptable at 90 km/h.

The decrease of TLC according to the relative yaw angle is now examined for a fixed speed $v = 90$ km/h (Fig. 6). The solid line corresponds to the vehicle located on the lane centerline while the dashed line corresponds to the vehicle center of gravity at 20 cm from the centerline to the left. When the vehicle is on the centerline, a TLC of 2.4 s is obtained when the relative yaw angle is $1°$.

One can notice that TLC decreases quickly and is less than 1 s beyond $2°$ of relative yaw angle. Furthermore, the effect of lateral displacement is more important for small values of ψ_L.
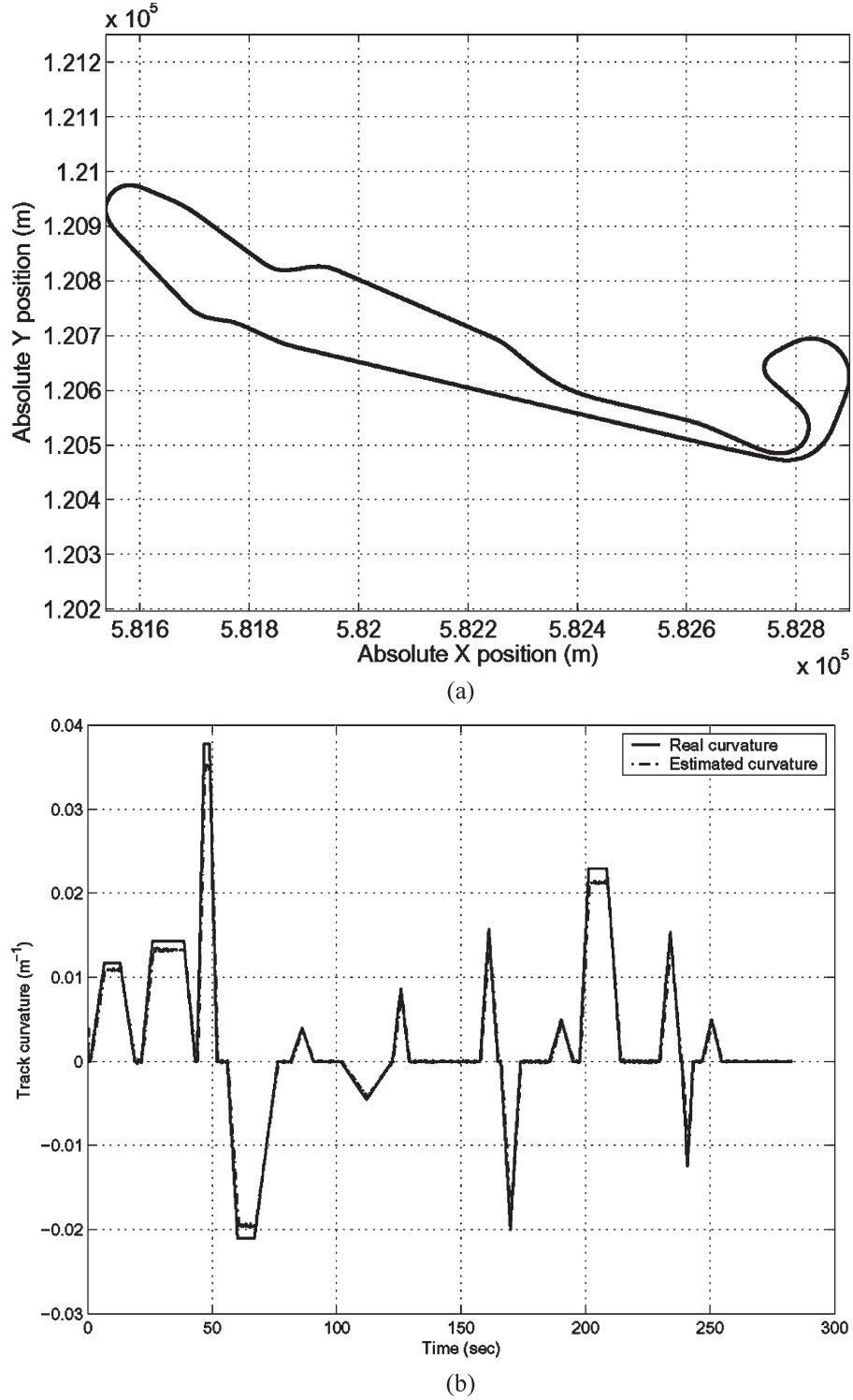
Fig. 8.   (a) Digitalized map of the Laboratoire sur les Interactions Véhicule-Infrastructure-Conducteur (LIVIC) test track. (b) Real and estimated track curvatures.

For fixed speed and relative yaw angle, TLC is proportional to y_{Gl}. As an example, a lateral displacement of 0.5 m leads to a TLC of only 2.25 s for $v = 90$ km/h and $\psi_L = 1°$.

B. Analysis With Nonzero Steering Angle on Straight Road Section

From the kinematic model, the steady-state value of the lateral acceleration is related to longitudinal speed and steering angle by

$$\gamma_l = \frac{v^2}{l_f + l_r} \tan \delta_f. \tag{33}$$

In the following, the steering angle is chosen according to speed value such that $\gamma_l = 3$ m/s^2. The radius of curvature of the vehicle path is computed from the stationary equality $(R_{v_l}^{-1} = \gamma_l/v^2)$.

We first assume that the relative yaw angle is zero. In this case, TLC is obtained from $t_{\mathrm{LC}} = (R_{v_l}/v) \cos^{-1}((R_{v_l} - y_{ll})/R_{v_l})$. Results obtained when varying the speed show that TLC is almost constant if the lateral acceleration is maintained constant. This suggests that lateral acceleration can be locally used as an indicator of the TLC. On the other hand, one can also deduce from the previous equation which is the maximal lateral acceleration achieving a TLC of 2 s. Assuming a 20-cm lateral displacement of CG, the obtained lateral acceleration is $\gamma_l = 4.2 \text{ m/s}^2$.

Finally, simulations show that a nonzero relative yaw angle leads to a linear decrease of TLC as the speed increases. The slope is almost proportional to the relative yaw angle.

C. Analysis on Curved Road Sections

It has been shown previously (Table III) that lane departure on the left side is avoided provided that $\psi_L < \psi_{tl} = \cos^{-1}(R_r/(R_r + y_{ll}))$. Fig. 7(a) gives the limit values for ψ_L as a function of y_{ll} for different values of curve radius R_r.

The corresponding TLC limit is shown in Fig. 7(b) for a speed of 90 km/h. It is obtained on a curved road section assuming a straight vehicle trajectory with initial relative yaw angle ψ_{tl}. One can notice that for highway curvatures, the relative yaw angle has to be under 5° to ensure a TLC of more than 2 s.

D. Simulation-Based Evaluation on Test Track Profile

In 1999, INRETS established a test track in Satory, 20 km west of Paris. The site is 3.5 km long with various road profiles including straight lane, tight bend, and squabble [Fig. 8(a)]. The lane markers' absolute positions were digitalized each 5 cm using differential GPS (DGPS). In addition, an experimental vehicle is equipped with video cameras on each side, which can detect lane markers at vehicle CG with high accuracy [6].

Fig. 8(b) shows the curvature of the track (solid line). The P2I observer developed above is able to estimate this curvature using only a video sensor (lateral displacement and relative yaw angle measurement) and the gyro as shown in Fig. 8(b). Fig. 9(a) gives a zoom of the estimation between time instants 110 and 190 s. For better precision with the lateral positioning, the lateral displacement is measured with two vertical cameras at the vehicle center of gravity. Fig. 9(b) shows that the observer is able to estimate the curvature derivative. The results obtained with the observer permit to trust that the DLC-based computation of the TLC can be implemented in near the future without use of DGPS and digitalized maps if the lane edges are of sufficient quality to be detected by video sensors.

Fig. 10(a) characterizes the test track in terms of DLC, when it is assumed that the vehicle is positioned on the centerline with zero relative yaw angle. This distance is greater than 300 m and reaches 900 m on the straight sections of the track (see Fig. 8(b) for the corresponding curvature). However, DLC is several times under 100 m, which means that small TLC values may be expected for high speeds or when lat-
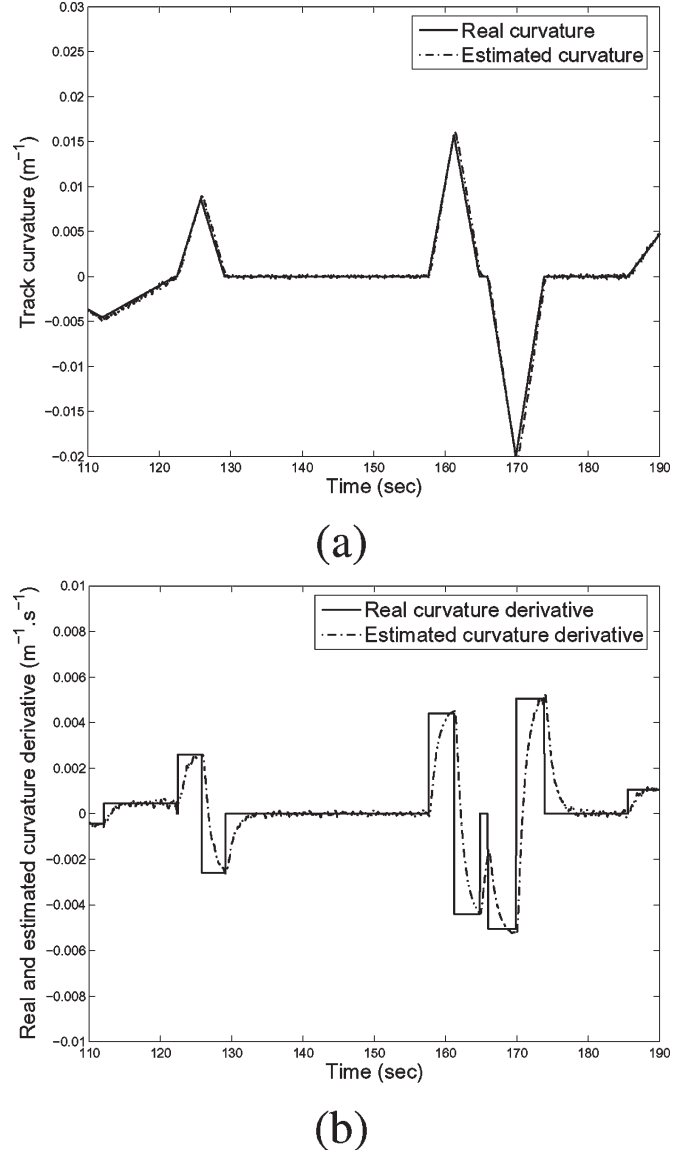

(a)

(b)

Fig. 9.   (a) Zoom on the real and estimated track curvatures. (b) Real and estimated curvature derivatives.

eral positioning or relative yaw angle errors are taken into account.

Speed is intentionally limited to 144 km/h (40 m/s) on straight sections, while on a curved section the forward speed is chosen to obtain a constant lateral acceleration of 0.3 g. The obtained speed profile is used in various forms in all TLC computations. Evaluation will be performed on the section from arc length 1500 m until the end of the track [Fig. 10(b)].

First, the vehicle is considered at the center of the lane with zero relative yaw angle. The TLC values are shown in Fig. 11(a).

The steering angle is now chosen at a nominal value according to (7) to obtain a vehicle radius path equal to the track curvature at a vehicle location. The TLC results are shown in Fig. 11(b). TLC is particularly enhanced on curved sections.

Vehicle relative lateral displacement is introduced of the form of a sinusoidal wave with 20-cm magnitude. Results are
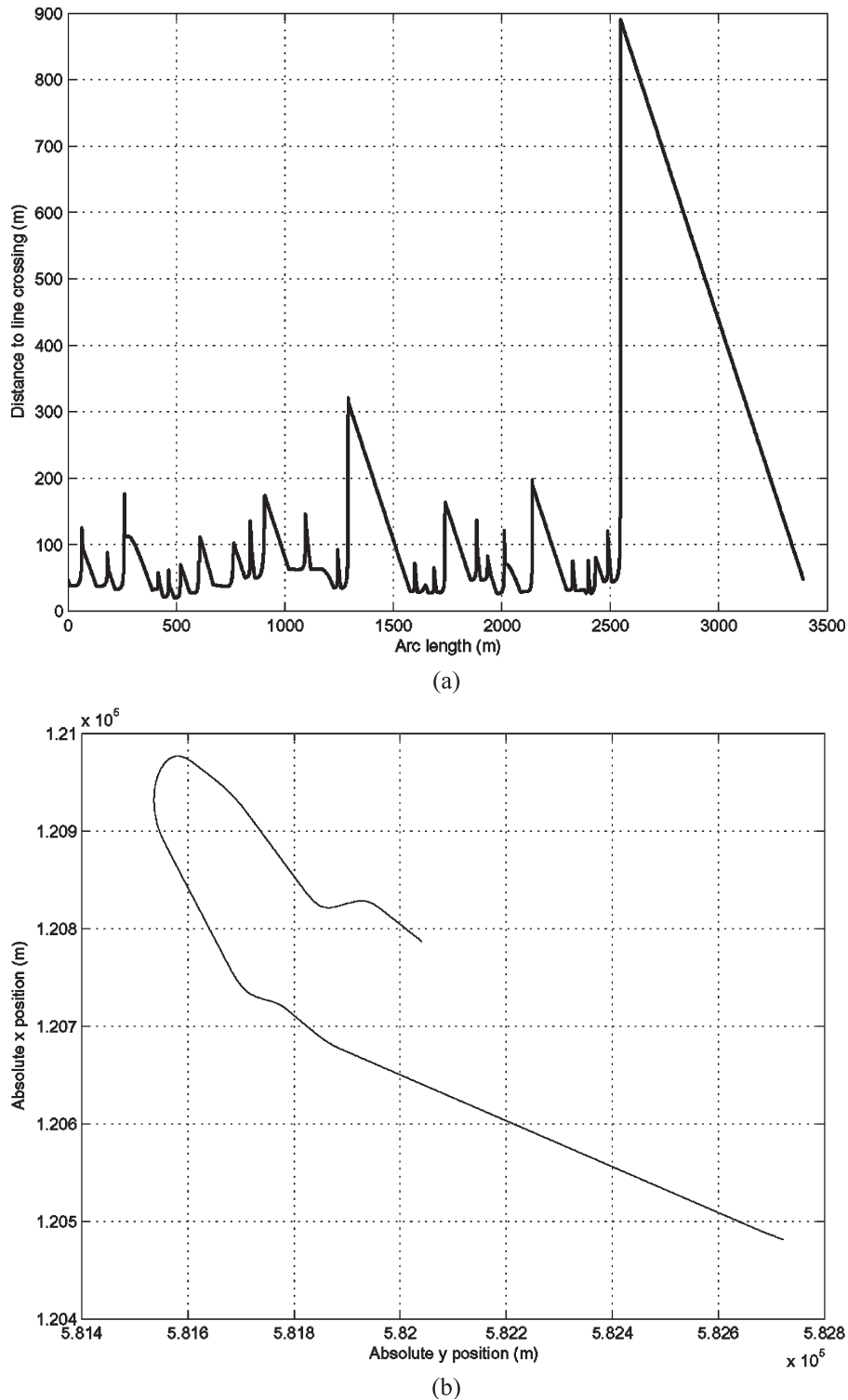
(a)

(b)

Fig. 10. (a) DLC along the track when it is assumed that the vehicle is positioned on the centerline with zero relative yaw angle. (b) Section of track on which TLC is computed.

provided in Fig. 11(c). The effect on TLC is only visible in the region between the two vertical bars.

A supplementary Gaussian random relative yaw angle error is also introduced. Variance is chosen at $1°$ and the obtained TLC is shown in Fig. 11(d). One can notice that high degradation of TLC values especially on the straight section.

VI. EXPERIMENTAL VALIDATION

In the previous sections, we have discussed the theoretical computation of the approximations of TLC. In practice, two classes of hypotheses could be used in the computation of the TLC.

The first class is about road consideration. It depends on the road sensor available in the vehicle. With only a short range
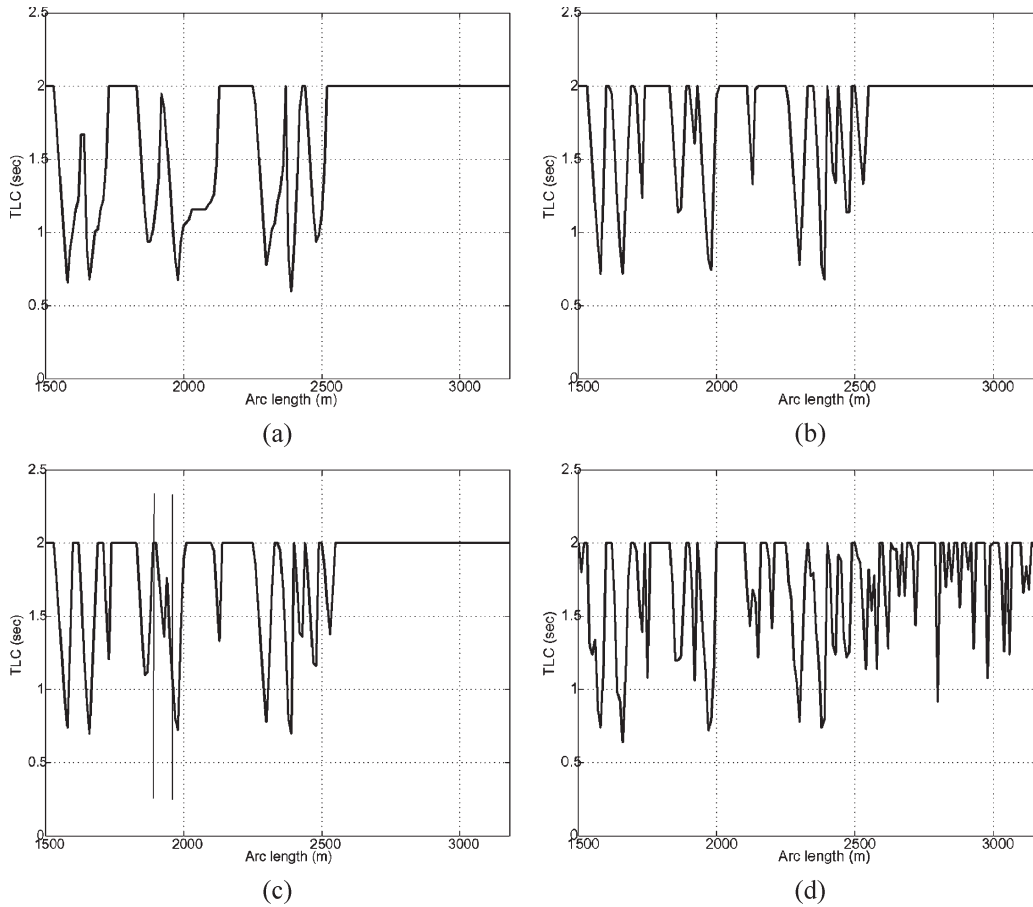
Fig. 11. (a) TLC values for vehicle on centerline with zero relative yaw angle and zero steering angle. The lateral acceleration is 0.3 g. (b) TLC values for vehicle on centerline with zero relative yaw angle and nominal steering angle. The lateral acceleration is 0.3 g. (c) Vehicle within 20 cm from the centerline of the lane, zero relative yaw angle, and nominal steering angle. The lateral acceleration is 0.3 g. (d) Vehicle within 20 cm from the centerline, Gaussian noise relative yaw angle, and nominal steering angle. The lateral acceleration is 0.3 g.

sensor, the road is considered as a straight line as we can only measure the lateral displacement and the road relative yaw angle. Long-range sensors give us knowledge of the road position, and we can fully take into account the road description.

The second class is relative to the vehicle knowledge. Without any sensor, we can make no assumption on the vehicle future path, so we consider it as a straight line. With sensors, such as a yaw rate sensor, speedometer, and steering angle, it is possible to predict the vehicle path for TLC computation. As mentioned before, advanced dynamic model prediction can be performed by the observer based state and curvature estimations.

Fig. 12 shows these different modes of TLC computations.

- In (a), the TLC is computed considering straight road approximation and straight vehicle trajectory (denoted LD/LD in future plots).
- In (b), the TLC is computed considering straight road approximation and curved vehicle trajectory (denoted LD/Ce).
- In (c), the TLC is computed considering real road profile and straight vehicle trajectory (denoted RR/LD).
- In (d), the TLC is computed considering real road profile and curved vehicle trajectory (denoted RR/Ce).

This set of figures shows the applied TLC computation on a curve. Consideration of the road in this case is very significant and leads to large variations in the TLC values.

The following parts will develop the experimental validation of the TLC computation. The main problem is to know which computation is the most efficient according to driving behavior.

This part is devoted to the definition of the experimental test to validate and compare the different TLCs. We present in the first subsection the sensors used for the TLC computation. We then explain the basic scenarios used for the validation of the TLC.

A. Sensors and Scenarios

To ensure a high accuracy on vehicle position and road description, we use a digital map and a centimeter real-time kinematic (RTK) GPS. These components are described below.

1) Digital Map: The maps, used for the experimental part, contain the position of the road edges and the center of the road. Positions are given with a longitudinal step of 50 cm, and the accuracy is about 1 cm.

2) GPS: To localize the vehicle on the map, an RTK GPS is used. The acquisition sampling frequency of the vehicle position is 20 Hz, and the accuracy is 1 cm due to the short
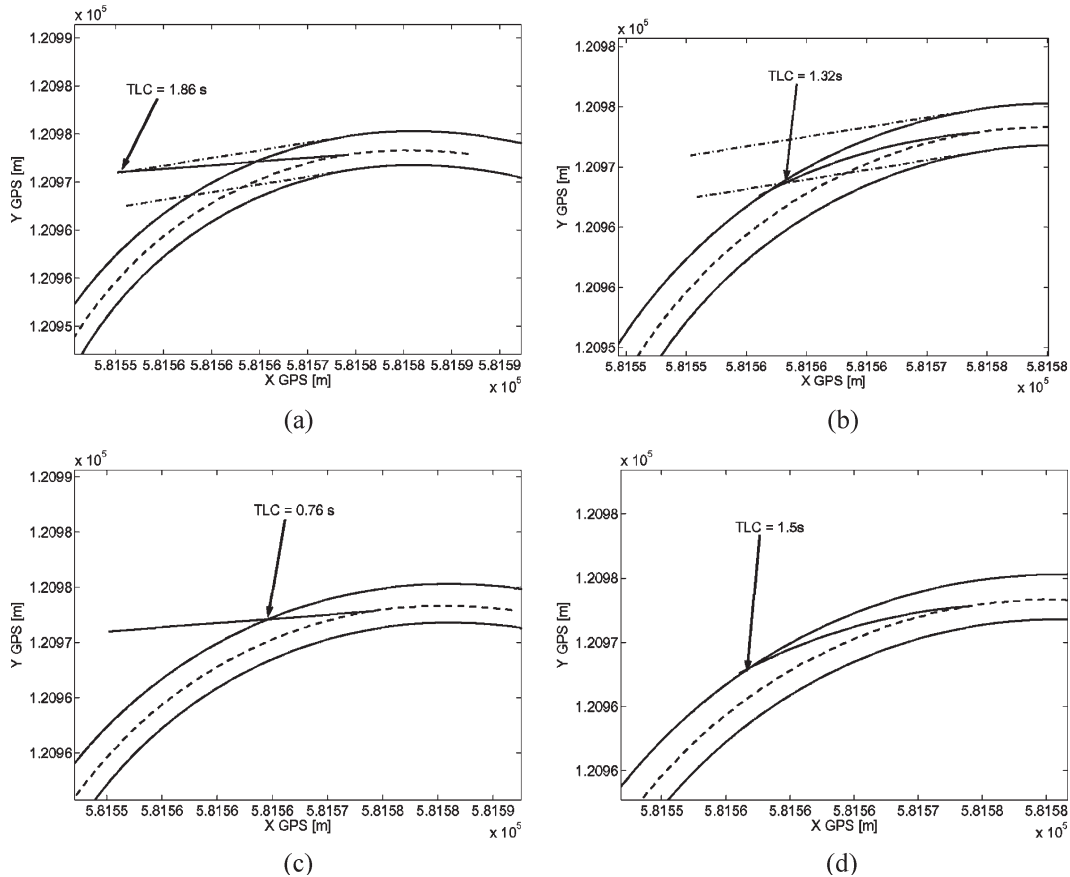
Fig. 12.   Different TLC approaches on a curve. (a) Straight road and vehicle trajectory approximations. (b) Straight road approximation and curved vehicle trajectory. (c) Real road profile and straight vehicle trajectory approximation. (d) Real road profile and curved vehicle trajectory.

TABLE VI
GPS ACCURACY VALIDATION

distance (cm)		lateral displacement (cm)		absolute
left	right	measured	rounded GPS	difference (cm)
83	63	-10	-9	1
70	76	3	3	0
78	68	-5	-5	0
79	67	-6	-6	0
50	96	23	24	1
64	82	9	9	0
67	79	6	6	0
89	57	-16	-16	0
81	65	-8	-9	1
64	82	9	10	1

distance to the base station. The accuracy of vehicle localization on the map using RTK GPS has been validated. This GPS was installed in a vehicle driving at about 50 km/h. The RTK GPS and the map have been used to compute the lateral displacement of the vehicle with respect to the center of the road. To validate this measure, lateral displacement was also computed using an external measure. This one was obtained by an experimental process that consisted of covering a part of the lane with sand and observing the marks that the vehicle left on this sand. Table VI summarizes ten measures of lateral displacement using both methods. All measures are given in centimeters, the difference between the two methods being rather small, with a mean of 0.4 cm. The centimeter accuracy of the GPS and map system is then validated.

The GPS centimeter mode is available on a large part of the test track, presented previously. Data used to assess the centimetric precision on the test track have been recorded during a 1-week test. Measures have been taken from 9:00 in the morning to 19:00 under various conditions, with the vehicle speed reaching 20 m/s. More than 200 turns have been done. This long period ensures collecting data from various GPS satellite constellations. Data used in the next parts are taken on sections with centimetric positioning.

3) Scenario: The tested scenarios represent common driving situations with respect to lane departure problems. To validate the TLC approach, in the first scenario, the driver is asked to drive normally, following the center of the road. In this scenario, the TLC is expected to have normal values, with small variations. Two driver styles were chosen for this scenario: low and high speeds.

In the second scenario, we wanted to test the reaction of the TLC with respect to a driver correction during a slow lane departure situation. So, the vehicle goes slowly near the road mark, and the driver has to correct this situation.

Finally, in the last scenario, the driver must cross the lane.

B. Results

1) Normal Driving Condition: The driver is asked to follow the center of the road with an average speed of 50 km/h.

Two relevant situations are plotted in Fig. 13. A long straight line ending with a curve is shown in Fig. 13(a). Fig. 13(b)
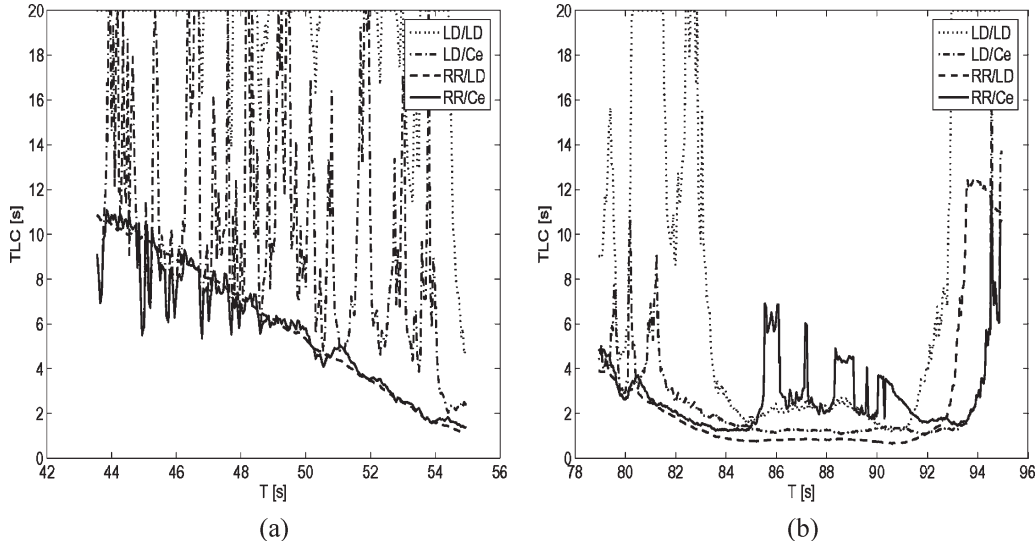
Fig. 13.   TLC variation during a normal driving scenario. (a) Drive on a straight line. (b) Drive on a curve.
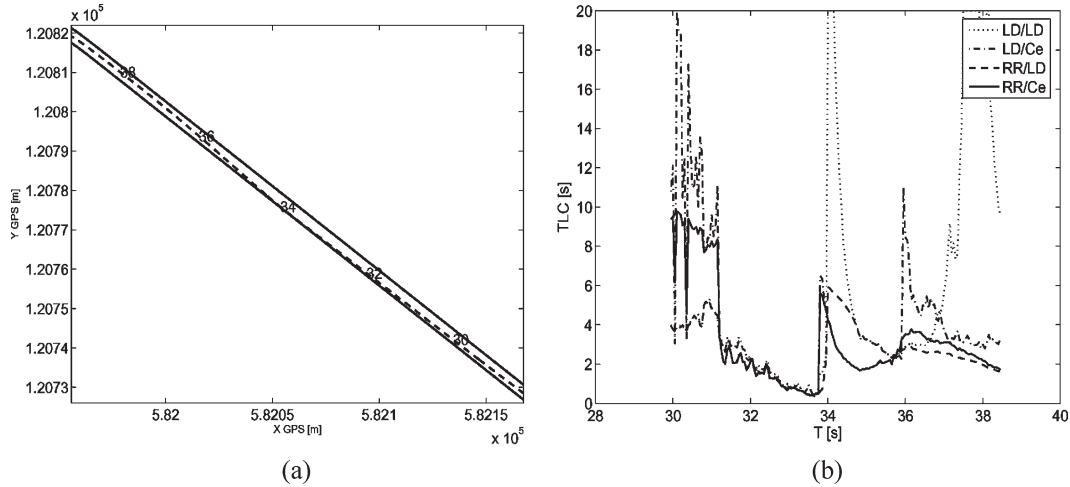

Fig. 14.   Slow road departure and driver correction scenario. (a) Vehicle trajectory. (b) Related TLC variation.

represents the values of the TLC on a curve. The first remark is that the values of the TLC are not small, as the driver, in this test, does not take risk. On these two plots, the TLC computed using the approximation of straight road may lead to large values and large variations of TLC. Since in this case the driver follows the center of the road, his relative yaw angle is small. As these approximations of the TLC are strongly dependent on this angle, a small variation of this variable has a large impact. On the other hand, information given using real road profile is reliable. On the straight line, the vehicle speed is approximately constant. So, his D_{LC} decreases with a constant speed. In the time versus time representation in Fig. 13(a), the slope of the TLC for these two approximations is near 1.

2) Slow Road Departure and Driver Correction: In this scenario, the driver goes near the lane marks but never crosses them. Figs. 14 and 15 show the vehicle trajectory and the related TLC. In both figures, the driver has performed a correction after a slow lane departure, which is the greater cause of lane departures.

With respect to Fig. 14, all TLC computations show good response to this problem. Values of different computations are similar: in this case, both road profile and vehicle trajectory are about a straight line before the driver correction. Moreover, the DLC is small. So, the different approximations on the vehicle trajectory and on the road profile lead to similar results. By using the curvature of the trajectory, the reaction in the TLC increase as a consequence of driver correction is 0.3 s faster than with the straight trajectory approximation.

In Fig. 15, excluding the TLC computed with straight road and straight trajectory approximations, all computations show a risky situation, with small TLC values (below 2 s and even 1 s). If we do not take into account the curvature of the trajectory in the TLC computation, we can see that the TLC does not reflect quite well the vehicle movement approaching the road marks. Moreover, the computation using real road profile and straight driver trajectory shows false variations: just before $T = 56$ s, the driver corrects his trajectory and moves away from the road mark, but the TLC value does not stop decreasing.
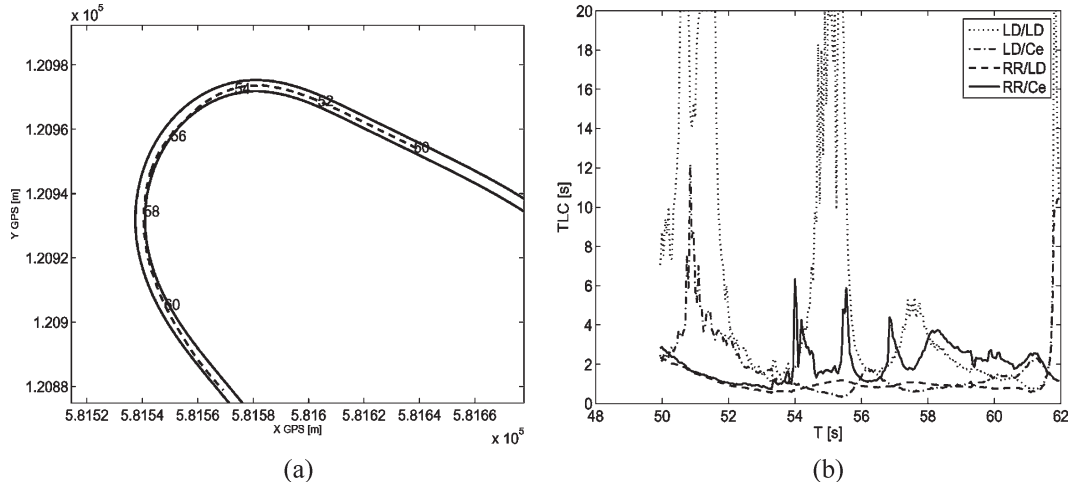
Fig. 15.   Slow road departure and driver correction scenario. (a) Vehicle trajectory. (b) Related TLC variation.
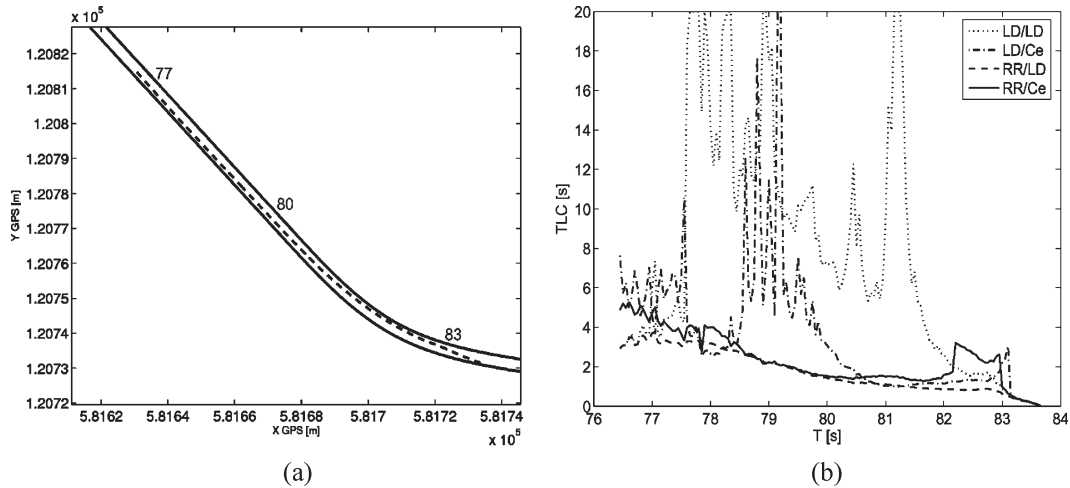

Fig. 16.   Road departure and driving scenario. (a) Vehicle trajectory. (b) Related TLC variation.

3) Road Departure: In this last scenario, the driver runs off the road. This road departure case simulates the loss of control, for instance, on an icy road.

Fig. 16 shows the vehicle trajectory and the TLC values. All TLC computations drop to zero when the vehicle crosses the road mark. Since the vehicle speed is constant, the slope of the TLC is near 1. The computation, using the vehicle trajectory curvature and the real road, shows a step of 1 s in TLC, 2 s before the lane departure. This step is due to driver correction. The TLC computation using both straight line approximations shows bad results as the TLC values, 2 s before the lane crossing, are very high and not representative of the emergency of the situation.

Developing a lane departure unit is a big challenge for accident and death reductions. The lane departure prevention unit has to provide information or an alarm to the driver that takes into account several constraints:

- excessive speed even on straight road section;
- vehicle positioning: excessive lateral displacement and excessive relative yaw angle;
- excessive lateral acceleration;
- small TLC values.

Decision making strategies for lane departure systems have been investigated by several authors [19], [22]. A lane departure warning unit that takes into account the fourth item is under validation [23].

VII. CONCLUSION

In this paper, TLC computation is presented on the basis of geometric kinematic formula and dynamic trajectory prediction. It is pointed out that all necessary data can be easily measured by a video sensor or DGPS, or estimated by using a model-based observer. Parameter effects analysis shows that the choice of one computation approximation for TLC is conditioned by the driving situation type and road characteristics. High accuracy measure of vehicle positioning is also needed particularly in terms of relative yaw angle. Experimental validation has not clearly highlighted one TLC computation as the best, but has allowed us to draw aside the straight road approximation. In fact, this approximation brings a too large variation in the TLC values and gives us TLCs that are not representative of the situation. This approximation has been considered to take into account sensor capacity: as a matter

of fact, it is easier to obtain the road profile at the location of the vehicle rather than in front of the vehicle. Using the real road profile, the approximation on vehicle trajectory leads to different results. With a straight vehicle trajectory, the TLC plot is smooth and presents good characteristics, but, compared to the curved trajectory, the reaction to driver correction is delayed. This study represents the first step in the use of TLC as a driver risk indicator. We have carried it out using an RTK GPS and an accurate map. To be largely used, the TLC implementation must require more common sensors, such as camera-based lane detection as well as cooperative systems or the use of observer-based methods.

REFERENCES

[1] J. Ackermann *et al.*, "Linear and nonlinear controller design for robust automatic steering," *IEEE Trans. Control Syst. Technol.—Special Issue on Automotive Control*, vol. 3, no. 1, pp. 132–143, Mar. 1995.

[2] K. T. Feng, "Look-ahead human machine interface for assistance of manual vehicle steering," in *Proc. Amer. Control Conf.*, 1999, pp. 1228–1232.

[3] K. T. Feng, H. S. Tan, and M. Tomizuka, "Future predictor for vehicle steering guidance—Sensitivity analysis and experimental results," in *Proc. Conf. Decision Control*, 1999, pp. 3722–3727.

[4] J. J. Gibson, *The Perception of The Visual World*. Boston, MA: Houghton Mifflin, 1950.

[5] H. Godthelp, P. Milgram, and G. J. Blaauw, "The development of a time related measure to describe driving strategy," *Hum. Factors*, vol. 26, no. 3, pp. 257–268, Jun. 1984.

[6] S. S. Ieng and D. Gruyer, "Merging lateral cameras information with proprioceptive sensors in vehicle location gives centimetric precision," in *Proc. ESV*, Nagoya, Japan, 2003. [CD-ROM].

[7] D. Koenig and S. Mammar, "Design of proportional-integral observer for unknown input descriptor systems," *IEEE Trans. Autom. Control*, vol. 47, no. 12, pp. 2057–2062, Dec. 2002.

[8] C.-F. Lin, A. G. Ulsoy, and D. J. LeBlanc, "Vehicle dynamics and external disturbance estimation for vehicle path prediction," *IEEE Trans. Control Syst. Technol.*, vol. 8, no. 3, pp. 508–518, May 2000.

[9] C. F. Lin and A. G. Ulsoy, "Time to lane crossing calculation and characterization of its associated uncertainty," *ITS J.*, vol. 3, no. 2, pp. 85–98, 1996.

[10] D. R. Mestre, "Dynamic evaluation of the useful field of view in driving," in *Proc. Driving Assessment*, 2001, pp. 234–239.

[11] I. Milleville-Pennel, J. M. Hoc, and F. Mars, "Useful sensory information for trajectory control while taking a bend," IRCCyN—UMR CNRS—Equipe PsyCoTec, Nantes, France, 2004. Internal Report R3-2004.

[12] B. J. Rogers and R. S. Allison, "When do we use optical flow and when do we use perceived direction to control locomotion?" *Perception*, vol. 28, no. Supplement 2, 1999.

[13] W. Van Winsum, K. A. Brookhuis, and D. de Waard, "A comparison of different ways to approximate time-to-line crossing (TLC) during car driving," *Accident Anal. Prev.*, vol. 32, no. 1, pp. 47–56, Jan. 2000.

[14] W. V. Van Winsum and H. Godthelp, "Speed choice and steering behavior in curve driving," *Hum. Factors*, vol. 38, no. 3, pp. 434–441, Sep. 1996.

[15] W. V. Van Winsum, D. de Waard, and K. A. Brookhuis, "Lane change maneuvers and safety margins," *Transp. Res., pt. F*, vol. 2, no. 3, pp. 139–149, 1999.

[16] P. H. Batavia, "Driver-adaptive lane departure warning systems," Ph.D. dissertation, Robot. Inst., Carnegie Mellon Univ., Pittsburgh, PA, 1999.

[17] P. H. Batavia, D. Pomerleau, and C. Thorpe, "Predicting lane position for roadway departure prevention," in *Proc. IEEE Intell. Vehicles Symp.*, 1998, pp. 5–10.

[18] M. Chen, T. Jochem, and D. Pomerleau, "AURORA: A vision-based roadway departure warning system," in *Proc. IEEE Conf. Intell. Robots Syst.—Human Robot Interaction and Cooperative Robots*, 1998, pp. 243–248.

[19] W. Kwon, J. W. Lee, D. Shin, K. Rob, D. Y. Kim, and S. Lee, "Experiments on decision making strategies for a lane departure warning system," in *Proc. IEEE Int. Conf. Robot. Autom.*, 1999, pp. 2596–2601.

[20] N. Mudaliar, D. LeBlanc, and H. Peng, "Linear estimator for road departure warning systems," in *Proc. Amer. Control Conf.*, 2004, pp. 2104–2109.

[21] D. B. Pape, V. K. Narendran, M. J. Koenig, J. A. Hadden, and J. H. Everson, "Dynamic vehicle simulation to evaluate countermeasure systems for run-off-road crashes," in *Proc. SAE Int. Congr. 81 Expo.*, Detroit, MI, 1996, pp. 400–409.

[22] S. Lee and W. Kown, "Performance evaluation of decision making strategies for an embedded lane departure warning system," *J. Robot. Syst.*, vol. 19, no. 10, pp. 499–509, Oct. 2002.

[23] C. Sentouh, S. Glaser, and S. Mammar, "Lane departure warning unit, design and evaluation," in *Proc. IV Symp.*, 2006. submitted for publication.

Saïd Mammar (M'97) received the Dipl.-Ing. degree from the École Supérieure d'Électricité, Gif-sur-Yvette, France, in 1992, the Ph.D. degree in automatic control from the Université Paris XI-Supelec, Orsay, France, in 1992, and the Habilitation to Direct Research (HDR) degree from the Université d'Evry, Evry, France, in 2001.

From 1992 to 1994, he held a research position at INRETS, the French National Institute on Transportation Research and Safety, France, where he worked on traffic network control. From 1994 to 2002, he was an Assistant Professor at Université d'Évry. He is currently a Professor and the Head of the Department of Electrical Engineering at Université d'Évry. He is currently involved in the integrated European Project PReVENT. His actual research interests include robust control, vehicle longitudinal and lateral control for driving assistance, and intelligent transportation systems.

Sébastien Glaser received the Dipl.-Ing. degree from the École Nationale des Travaux Publics de l'État, Lyon, France, in 2001, the M.S. degree in vision from the University of Saint Étienne, France, in 2001, and the Ph.D. degree in automatic control from the University of Évry, Evry, France, in 2004.

Since 2001, he has been with the INRETS/LCPC-Laboratoire sur les Interactions Véhicule-Infrastructure-Conducteur, Versailles, France. He is currently involved in the Integrated European Projects SafeSpot and Co-operative Vehicle-Infrastructure Systems (CVIS). His actual research interests include intelligent transportation systems, vehicle modeling, and control with driver interaction.

Mariana Netto received the B.Sc. degree in electronic engineering and the M.Sc. degree in automatic control from the Federal University of Rio de Janeiro, Brazil, in 1995 and 1997, respectively, and the Ph.D. degree in automatic control from the Laboratoire des Signaux et Systémes (L2S)-Supélec-Université Paris Sud, France, in 2001.

She is currently a Researcher at the INRETS/LCPC-Laboratoire sur les Interactions Véhicule-Infrastructure-Conducteur, Versailles, France. She is currently involved in the Integrated European Project PReVENT. Her research interests include nonlinear and adaptive control, full and shared lateral control for driver assistance systems, and intelligent transportation systems.